

Relaxation rate of ModMax-de Sitter black holes perturbed by massless neutral scalar fields

Haryanto M. Siahaan*

Jurusan Fisika, Universitas Katolik Parahyangan,
Jalan Ciumbuleuit 94, Bandung 40141, Indonesia

Abstract

In this study, we investigate the behavior of ModMax-de Sitter black holes when perturbed by massless neutral scalar fields. Specifically, we analyze how the relaxation time, defined as the inverse of the fundamental imaginary frequency, varies with respect to two key parameters: the cosmological constant and the nonlinear parameter characterizing the ModMax theory. We explore scenarios both with and without a cosmological constant, focusing on the static charged ModMax black hole configuration. Our results reveal dependencies between the relaxation time and the nonlinear parameter, shedding light on the dynamical properties of these black hole systems. We also show the validity of WKB approximation under consideration.

arXiv:2409.03359v1 [gr-qc] 5 Sep 2024

*haryanto.siahaan@unpar.ac.id

1 Introduction

Born and Infeld were pioneers in proposing a model for non-linear electrodynamics (NED) known as Born-Infeld (BI) theory [1]. Their motivation stemmed from addressing the inherent divergences within Maxwell's theory, particularly at short distances. In BI NED, the self-energy of charges remains finite, and the effective action can be derived from open superstrings, offering a framework devoid of physical singularities [2]. Another example of NED is Euler-Heisenberg (EH) theory, which arises from vacuum polarization [3]. Both BI NED and EH NED converge to Maxwell's electrodynamics in the weak field regime.

Recently, in [4], the authors introduced a generalization of Maxwell electrodynamics termed ModMax electrodynamics, characterized by a single dimensionless parameter. The static electrically charged black hole solution in the Einstein-ModMax theory was introduced in [5], closely resembling the well-known Reissner-Nordstrom solution but incorporating a screening factor that shields the actual black hole electrical charge. This new charged black hole solution has garnered attention from various authors exploring its diverse aspects [6, 7, 8, 9, 10, 11, 12, 13, 14, 15].

Quasinormal modes (QNMs) describe the damped oscillations observed in a black hole or field system when it encounters perturbations [16]. These modes become particularly prominent during the final stages of a black hole merger, appearing as gravitational waves. Research into QNMs has a history spanning over five decades, with recent interest focusing on their relevance to the Penrose strong cosmic censorship conjecture [17, 18] and the black hole's no-hair theorem [19, 20, 21, 22, 23, 24, 25, 26]. QNMs, considered as linear perturbations, are typically represented as $e^{-i\omega t}$, where t denotes time and ω is the complex quasinormal resonance spectrum function [27, 28, 29]. The imaginary part of ω contributes to damping, while the real part indicates the oscillation of the perturbation. Physically, the spectrum function should exhibit purely ingoing behavior at the black hole's horizon and purely outgoing behavior at spatial infinity for asymptotically flat or de Sitter (dS) spacetime (or finite behavior at spatial infinity for Anti-de Sitter (AdS) spacetime) [16], resulting in a discrete resonance spectrum denoted by $\omega = \omega_n$, with n representing the overtone number. Unstable perturbations are characterized by $\text{Im}(\omega) > 0$.

The uniqueness theorem [30, 31, 32] posits that the Kerr-Newman black hole family in Einstein-Maxwell theory can have at most three conserved quantities: mass, electric charge, and angular momentum. This theorem supports the no-hair conjecture [33], asserting that perturbations of matter fields on black holes within the Einstein-Maxwell family will eventually dissipate over time. Consequently, the QNMs, describing the interaction between a black hole and external matter field, are primarily characterized by the damping resonance spectrum. However, recent numerical [34, 35] and analytical [22] studies have shown instability in the Reissner-Nordström (RN) black hole within an asymptotically de Sitter (dS) spacetime, under perturbations originating from charged scalar fields.

The relaxation time, inversely related to the fundamental quasinormal modes as $\tau = \omega_I^{-1}(n = 0)$, serves as a characteristic quantity reflecting the rate at which perturbations affecting the black hole by the matter field dissipate. Previous studies have explored the relaxation time of the RN black hole perturbed by charged massive scalar fields [36, 37], as well as the relaxation rate for the combined RN black hole/massless scalar field system [38, 39]. In this paper, we investigate the relaxation time of the static charged ModMax black hole in de Sitter space perturbed by a neutral massless scalar field. The analytical quasinormal resonance frequency for the system is presented in the eikonal regime. We also examine the influence of cosmological constant and non-

linear parameters to the relaxation time. In addition to these works, we also present the fastest relaxation rate of the black hole for the asymptotically flat space case, and how the non-linear parameter contributes to the rate.

The organization of this paper is as follows. In the next section we provide a brief review on ModMax black holes in de Sitter space. In section 3 we discuss the relaxation time in both de Sitter and asymptotically flat cases. Then we give a conclusion. In this paper, we consider natural units where $G = c = \hbar = 1$.

2 Black holes in Einstein-ModMax theory with cosmological constant

Let us start by reviewing some general properties of the ModMax black hole in de Sitter spacetime. The theory is described by Lagrangian

$$S = \frac{1}{16\pi} \int_{\mathcal{M}} d^4x \sqrt{-g} (R - 2\Lambda - 4\mathcal{L}_{\text{MM}}) \quad (2.1)$$

where the Lagrangian for ModMax electrodynamics is given by

$$\mathcal{L}_{\text{MM}} = -\mathcal{X} \cosh(v) + \sqrt{\mathcal{X}^2 + \mathcal{Y}^2} \sinh(v) . \quad (2.2)$$

In the last equation,

$$\mathcal{X} = \frac{1}{4} \mathcal{F}_{\alpha\beta} \mathcal{F}^{\alpha\beta} , \quad (2.3)$$

and

$$\mathcal{Y} = \frac{1}{4} \mathcal{F}_{\alpha\beta} \tilde{\mathcal{F}}^{\alpha\beta} , \quad (2.4)$$

where $\tilde{\mathcal{F}}_{\kappa\lambda} = \frac{1}{2} \varepsilon_{\kappa\lambda\alpha\beta} \mathcal{F}^{\alpha\beta}$ is the dual Maxwell field strength tensor $\mathcal{F}_{\alpha\beta} = \partial_\alpha A_\beta - \partial_\beta A_\alpha$. Note that causality requires $v \geq 0$ [4]. From this ModMax Lagrangian, we can construct the Plebanski dual variable

$$\mathcal{P}_{\alpha\beta} = \left(\cosh(v) - \frac{\mathcal{X}}{\sqrt{\mathcal{X}^2 + \mathcal{Y}^2}} \sinh(v) \right) \mathcal{F}_{\alpha\beta} - \frac{\mathcal{Y} \sinh(v)}{\sqrt{\mathcal{X}^2 + \mathcal{Y}^2}} \tilde{\mathcal{F}}_{\alpha\beta} . \quad (2.5)$$

The corresponding field equations in ModMax theory then can be written as

$$\nabla_\alpha \mathcal{P}^{\alpha\beta} = 0 . \quad (2.6)$$

Varying the action (2.1) with respect to metric tensor $g_{\mu\nu}$ yield the Einstein equations

$$R_{\alpha\beta} - \frac{1}{2} g_{\alpha\beta} R + \frac{3}{L^2} g_{\alpha\beta} = 8\pi T_{\alpha\beta} , \quad (2.7)$$

where the cosmological constant is $\Lambda = 3L^{-2}$ and the energy-momentum tensor is given by

$$T_\alpha^\beta = \frac{1}{4\pi} \left(\delta_\alpha^\beta \mathcal{L}_{\text{MM}} - \mathcal{F}_{\alpha\kappa} \mathcal{P}^{\kappa\beta} \right) . \quad (2.8)$$

In the study by Flores-Alfonso et al. [5], a family of dyonic static charged black hole solutions was derived, satisfying the equations of motion in ModMax theory coupled with Einstein gravity.

Essentially, the authors extended the dyonic Reissner-Nordström spacetime of Einstein-Maxwell theory to accommodate the Einstein-ModMax framework. The resulting solution resembles closely to the Reissner-Nordstrom metric, featuring a new term interpreted as a screening factor that shields the true charge of the black hole.

The ModMax black hole solution in de Sitter spacetime is discussed in [13, 6, 15]. The spacetime metric describing ModMax black hole in de Sitter spacetime can be written as

$$ds^2 = -Fdt^2 + F^{-1}dr^2 + r^2d\theta^2 + r^2\sin^2\theta d\phi^2, \quad (2.9)$$

where

$$F = 1 - \frac{2M}{r} + \frac{Q^2 e^{-v}}{r^2} - \frac{r^2}{L^2}. \quad (2.10)$$

The accompanying gauge vector is

$$A_\mu dx^\mu = \frac{Qe^{-v}}{r} dt. \quad (2.11)$$

Setting the non-linear (NL) parameter $v = 0$, which transforms the Einstein-ModMax theory to become just Einstein-Maxwell, the above metric reduces to the widely known Reissner-Nordstrom solution with mass M and electric charge Q .

Similar to the Reissner-Nordstrom-de Sitter spacetime, ModMax-de Sitter geometry also possesses the inner and outer black hole horizons, as well as the cosmological one. They come from the three positive roots of F above. Some numerical evaluations of the inner and outer black hole horizons for ModMax-de Sitter spacetime are given in fig. 2.2. It illustrates how changes in the non-linear parameter v influence the positions of the horizons, albeit with minimal impact on the cosmological horizon. However, it is important to note that our consideration of v in this figure is significant, whereas in reality, we should consider very small values for this parameter. Thus, we can conclude that the existence of non-linear parameters in regard to the profile of the metric function F does not change its general properties. It causes a slight shift in the locations of the black hole horizons and has an almost negligible impact on the position of the cosmological horizon. Therefore, in subsequent discussions, we often resort to the original Maxwell theory for numerical estimations to validate the WKB approximation employed in the following sections. Similar behavior is also observed in the Shark Fin diagram, which delineates extremalities in spacetime, as depicted in fig. 2.1. The non-linear parameters induce shifts in the curves corresponding to the cold and Nariai solutions, including the ultracold point.

Before we discuss the time relaxation for ModMax-de Sitter black hole, let us provide here some basics of its thermodynamics. The black hole temperature is given by

$$T_H = \frac{F'(r_+)}{4\pi} = \frac{1}{4\pi r_+} \left(1 - \frac{e^{-v}Q^2}{r_+^2} - \frac{3r_+}{L^2} \right), \quad (2.12)$$

whereas the entropy is related to its area in the standard a quarter area formula,

$$S = \frac{\text{Area}}{4} = \pi r_+^2. \quad (2.13)$$

The corresponding first law for black hole horizon is given by [13]

$$\delta M = T_H \delta S + \Phi_H \delta Q + V_H \delta P \quad (2.14)$$

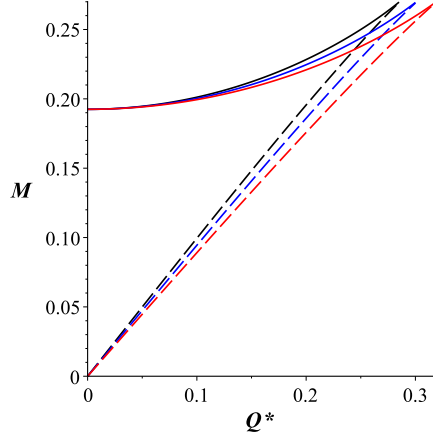


Figure 2.1: Cases $e^{-v} = 1$, $e^{-v} = 0.9$, $e^{-v} = 0.8$ are represented by the black, blue, and red curves, respectively. Here we consider $L = M$ and use the notation $Q^* = QM^{-1}$. Black hole states are represented by the area bounded by the dashed and solid curves. Dashed curves belong to cold black holes, whereas solid curves describe the Nariai case. The ultracold solutions are given by the intersection of solid and dashed curves for each v case.

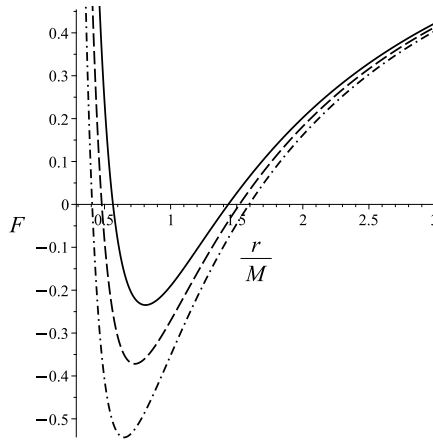


Figure 2.2: Evaluation of F function in eq. (2.10) with numerical setup $L = 100 M$ and $Q = 0.9 M$. Solid, dashed, and dashed-dot represent the cases of $e^{-v} = 1$, $e^{-v} = 0.9$, and $e^{-v} = 0.8$, respectively. For each curve, intersections at smaller radius denote the inner black hole horizon, whereas the larger ones correspond to the outer black hole horizon. For the three curves, the cosmological horizons almost overlap at $r \approx 98.99 M$.

where

$$\Phi_H = -\frac{Qe^{-v}}{r_+}, \quad (2.15)$$

$$V_H = \frac{4}{3}\pi r_+^3, \quad (2.16)$$

and

$$P = -\frac{3}{8\pi L^2} \quad (2.17)$$

are the electric potential at horizon, thermodynamic volume, and the dynamical pressure, respectively. Accordingly, the related Smarr relation can be shown as

$$M = 2T_H S + \Phi_H Q - 2V_H P. \quad (2.18)$$

Indeed, it can be demonstrated that there exists a temperature linked to the cosmological horizon, which precisely follows the formula (2.12) when substituting r_+ with r_c . Consequently, one can also explore the entropy of the cosmological horizon along with the associated first law. However, for the scope of this paper, our focus remains on the dynamics of the test scalar field around the black hole, and thus certain aspects related to the cosmological horizon will not be further investigated.

3 Time relaxation

Quasinormal modes (QNMs) of black holes are oscillatory patterns that arise when a black hole is perturbed by external influences, such as gravitational waves or matter fields. These modes represent the characteristic frequencies at which the black hole "rings" after being disturbed, analogous to the vibrations of a bell after being struck. QNMs are characterized by complex frequencies, with a real part determining the oscillation frequency and an imaginary part determining the rate of decay or damping. The relaxation time, on the other hand, is a measure of how quickly perturbations to a black hole system dissipate or relax. It is defined as the inverse of the imaginary part of the fundamental quasinormal mode frequency, representing the timescale over which the perturbation dies away. In other words, the relaxation time quantifies how long it takes for the black hole to return to a stable, equilibrium state after being perturbed.

In this section, we derive the relaxation time for a ModMax-de Sitter black hole disturbed by a massless neutral scalar field. The relaxation time is computed as the reciprocal of the imaginary component of the scalar frequency at the lowest overtone number. Our analysis is conducted using the WKB approximation in the eikonal limit, where we assume a large spherical harmonic index, specifically $l \gg 1$. The Klein-Gordon equation governing the test scalar field is expressed as follows

$$\nabla_\mu \nabla^\mu \Phi(t, r, \theta, \phi) = 0. \quad (3.1)$$

The symmetry of spacetime allows us to consider the form

$$\Phi = \sum_{lm} \frac{R_{lm}(r)}{r} e^{-i\omega t} S_{lm}(\theta, \phi) \quad (3.2)$$

as the solution of the scalar field where m and ω are the azimuthal quantum number and frequency of the field, respectively. This ansatz for the wave function above leads to separable expressions for the wave equation (3.1).

The radial part of the Klein-Gordon equation reads

$$F^2 \frac{d^2 R}{dr^2} + \frac{dF}{dr} F \frac{dR}{dr} + UR = 0, \quad (3.3)$$

where

$$U = \omega^2 - \frac{F^2}{r^2} - \frac{K_l F}{r^2} - \frac{rF}{r^2} \frac{dF}{dr} \quad (3.4)$$

and $K_l = l(l+1)$. Now let us consider the tortoise coordinate y where

$$dy = \frac{dr}{F}. \quad (3.5)$$

It yields the reading of radial equation (3.3) becomes

$$\frac{d^2 R}{dy^2} + ZR = 0 \quad (3.6)$$

where

$$Z = \omega^2 - F \left(\frac{K_l}{r^2} - \frac{2r^2}{L^2} + \frac{2M}{r^3} - \frac{2Q^2 e^{-v}}{r^4} \right). \quad (3.7)$$

For the scalar field perturbation, we consider the purely ingoing mode at the horizon and purely outgoing at the spatial infinity. Accordingly, the proper boundary conditions that can be employed are

$$R(r \rightarrow r_+) \sim e^{-i\omega y}, \quad R(r \rightarrow r_c) \sim e^{i\omega y}. \quad (3.8)$$

Such conditions lead to the distinction of quasinormal resonant modes which characterize the relaxation dynamics of the massless scalar fields in the black hole background.

Now let us consider the eikonal regime $K_l \gg 1$, hence

$$Z \sim \omega^2 - \frac{K_l F}{r^2}. \quad (3.9)$$

The extremum of the last expression can be located at r_0 where

$$\left. \frac{dZ}{dr} \right|_{r=r_0} = 0. \quad (3.10)$$

It can be found that the radius r_0 obeying the last equation is

$$r_0 = \frac{3M}{2} + \frac{1}{2} \sqrt{9M^2 - 8Q^2 e^{-v}}, \quad (3.11)$$

where interestingly it does not depend on the cosmological constant Λ . As expected, the value of r_0 above reduces to the corresponding radius in Reissner-Nordstrom [38] case after taking v to be zero.

The WKB equation to obtain the resonance frequencies are given by [40, 41, 38]

$$\frac{Z_0}{\sqrt{2Z_0^{(2)}}} = -i \left(n + \frac{1}{2} \right) + \dots \quad (3.12)$$

where the ellipses represent terms that can be disregarded². In the final equation, we have employed the notation $Z_0 = Z(r_0)$ and

$$Z_0^{(k)} = \left. \frac{d^k Z}{dy^k} \right|_{r=r_0}. \quad (3.13)$$

²We will revisit these disregarded terms in the subsequent section where we demonstrate the validity of the approximation made in this computation.

For the case of black hole being discussed here, one can show the corresponding WKB resonance frequencies equation is

$$\omega^2 - \frac{K_l F_0}{r_0^2} = -i \left(n + \frac{1}{2} \right) F_0 \left[2K_l \left(\frac{4}{r^3} \frac{dF}{dr} - \frac{1}{r^2} \frac{d^2 F}{dr^2} - \frac{6F}{r^4} \right) \right]_{r=r_0}^{1/2}. \quad (3.14)$$

Recalling that the relaxation time is associated with the damping mode of the scalar field, we consider $\omega = \omega_R - i\omega_I$, where ω_R and ω_I are both positive. Taking the square of both sides in eq. (3.14) and imposing the condition $\omega_R \ll \omega_I$, we can demonstrate that

$$\omega_R \sim l \frac{\sqrt{F_0}}{r_0}, \quad (3.15)$$

and

$$\omega_I \sim \frac{(1 + 2n) r_0 \sqrt{2F_0 Z_0^{(2)}}}{4\sqrt{K_l}}. \quad (3.16)$$

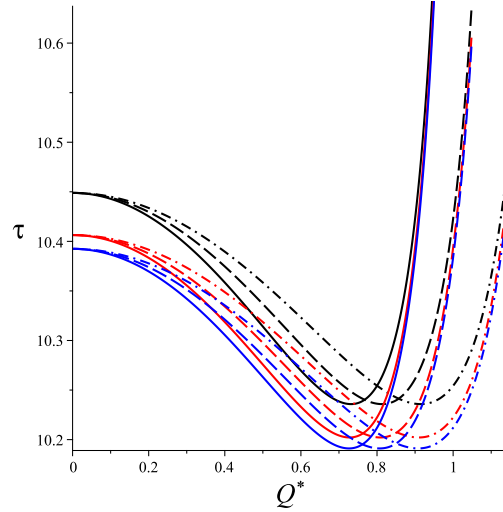


Figure 3.1: The blue, red, and black curves represent the cases $L^* = 50$, $L^* = 100$, and $L^* = 1000$. Within each case, the solid, dashed, and dashed-dot curves represent $v = 0$, $v = -\ln 0.9$, and $v = -\ln 0.8$, respectively.

Now, the imaginary part of scalar's frequency in eq. (3.16) will give us the relaxation time of the scalar field near the black hole horizon. The time relaxation is given by the inverse of ω_I at the fundamental mode $n = 0$, i.e.

$$\tau = \frac{L^* (3 + \mu)^3}{2 \{ [(3 + \mu - 2Q^{*2}e^{-v}) L^{*2} - 27\mu + 72Q^{*2}e^{-v} + 12\mu Q^{*2}e^{-v} - 81 - 8Q^{*4}e^{-2v}] [3\mu - 8Q^{*2}e^{-v} + 9] \}^{1/2}} \quad (3.17)$$

where $\mu = \sqrt{9 - 8Q^{*2}e^{-v}}$. From this point forward, starred quantities represent the dimensionless versions of their respective quantities obtained by dividing them by the black hole mass M .

In fig. 3.1, some numerical evaluations of the relaxation time above are provided. The plots reveal that for specific parameters Q and v , the relaxation time increases as the cosmological constant decreases. Such behavior is consistent with that observed in the Reissner-Nordstrom-de Sitter spacetime [42]. Additionally, the influence of the non-linear parameters on the relaxation time is evident in Figure 3.1. With an increase in v , the curve's minimum point shifts towards larger values of Q . This observation is expected, given that the non-linear parameter v acts to shield the actual electrical charge of the black hole.

Now, let us examine the scenario where there is no cosmological constant, leading to the simplification of the relaxation time (3.17) to:

$$\tau = \frac{(3 + \mu)^3}{2\sqrt{3\mu^2 + 2(9 - 7Q^2e^{-v})\mu - 42Q^2e^{-v} + 27}}, \quad (3.18)$$

The extremum of τ occurs as Q^* varies, situated at $Q^* \simeq 0.72636 e^{v/2}$, which exhibits a linear dependency on v within a very small range of v . In the limit as $v \rightarrow 0$, the fastest relaxation rate converges to 0.72636, consistent with the Reissner-Nordstrom case documented in [38]. Figure 3.2 visualizes the behavior of the relaxation time near its minimum value for various non-linear parameter values.

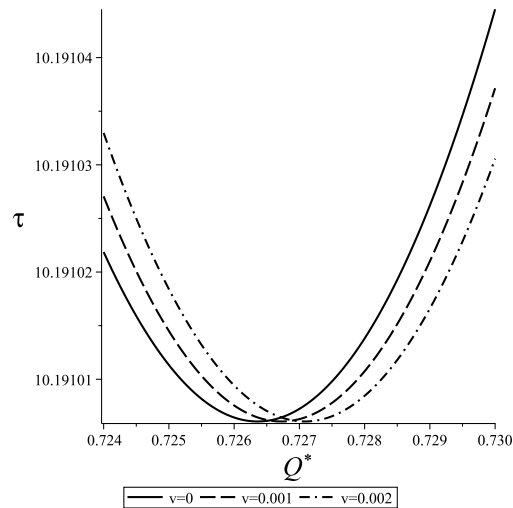


Figure 3.2: Numerical evaluations for τ in eq. (3.18) for several non-linear parameter cases. The solid, dashed, and dashed-dot curves correspond to $v = 0$, $v = -\ln 0.9$, and $v = -\ln 0.8$, respectively.

4 Checking of the WKB validity

In this section, we will validate the approximation utilized in deriving the WKB resonance condition (3.12), where certain terms in the equation warrant scrutiny. The expression (3.12), in its full form,

represents the Taylor expansion of Z from equation (3.6) around r_0 [40, 41]

$$\frac{iZ_0}{\sqrt{2Z_0^{(2)}}} = \alpha + \Pi_n + \Theta_n, \quad (4.1)$$

where

$$\Pi_n = \frac{1}{\sqrt{2Z_0^{(2)}}} \left[\frac{Z_0^{(4)} (1 + 4\alpha^2)}{32Z_0^{(2)}} - \frac{1}{288} \left(\frac{Z_0^{(3)}}{Z_0^{(2)}} \right)^2 (7 + 60\alpha^2) \right] \quad (4.2)$$

and

$$\Theta_n = \frac{\alpha}{2Z_0^{(2)}} \left[\frac{5(77 + 188\alpha^2)}{6912} \left(\frac{Z_0^{(3)}}{Z_0^{(2)}} \right)^4 - \frac{51 + 100\alpha^2}{384} \left(\frac{Z_0^{(3)}}{Z_0^{(2)}} \right)^2 \frac{Z_0^{(4)}}{Z_0^{(2)}} \right. \\ \left. + \frac{67 + 68\alpha^2}{2304} \left(\frac{Z_0^{(4)}}{Z_0^{(2)}} \right)^2 + \frac{19 + 28\alpha^2}{288} \frac{Z_0^{(3)} Z_0^{(5)}}{\left(Z_0^{(2)} \right)^2} - \frac{5 + 4\alpha^2}{288} \frac{Z_0^{(6)}}{Z_0^{(2)}} \right]. \quad (4.3)$$

In equations above, note that we have used

$$\alpha = n + \frac{1}{2}. \quad (4.4)$$

Furthermore, for the WKB potential in eq. (3.9) in the eikonal limit, we have

$$\Pi_n = \frac{\sqrt{2}}{288F_0\sqrt{K_l} \left(4F_0^{[1]}r_0 - 6F_0 - r_0^2F_0^{[2]} \right)^{3/2}} \sum_{j=0}^6 \beta_j r_0^j, \quad (4.5)$$

and

$$\Theta_n = -\frac{2n+1}{6912F_0K_l \left(4F_0^{[1]}r_0 - 6F_0 - r_0^2F_0^{[2]} \right)^5} \sum_{j=0}^{12} \gamma_j r_0^j, \quad (4.6)$$

where $F_0 = F(r_0)$ and

$$F_0^{[k]} \equiv \left. \frac{d^k F}{dr^k} \right|_{r_0}. \quad (4.7)$$

The complete expressions for β_j 's and γ_j 's are given in the appendix.

Note that the function $4F_0^{[1]}r_0 - 6F_0 - r_0^2F_0^{[2]}$ appearing in the denominator for Π_n and Ω_n has the result

$$4F_0^{[1]}r_0 - 6F_0 - r_0^2F_0^{[2]} = \frac{36 + 12\mu - 32e^{-v}Q^{*2}}{(3 + \mu)^2}$$

which remains finite within our specified range of interest, $0.8 \leq e^{-v} \leq 1$ and $0 \leq Q^* \leq 1$. Although certain terms in the series for Π_n and Ω_n may involve large numbers, numerical evaluations illustrated in figures 4.1, 4.2, and 4.3, conducted for the standard Maxwell case ($v = 0$), suggest that minor adjustments for v will not significantly alter the plot's characteristics. The modes of Π_n and Θ_n evaluated in 4.2 and 4.3 correspond to the fundamental ones, i.e., $n = 0$, as these are

crucial in determining the relaxation time if they are not negligible. The figures indeed indicate that Π_0 and Θ_0 can be safely disregarded in the eikonal limit. While the evaluations are performed only for several numerical values of the cosmological constant, we are confident that the assertion regarding the negligibility of Π_0 and Θ_0 in the eikonal limit applies more broadly. Therefore, we can confirm the validity of our WKB analysis on the relaxation time when considering the eikonal limit $K_l \gg 1$.

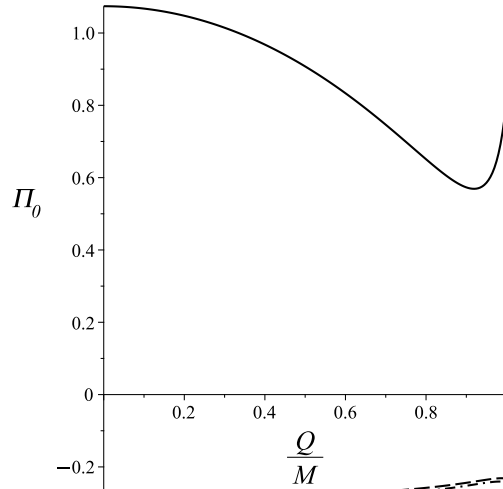


Figure 4.1: Here are numerical examples of Π_0 . The solid line represents $L = 1$, the dashed line represents $L = 10$, and the dashed-dot line represents $L = 100$. For higher L , the curves will nearly overlap with the $L = 100$ case. We focus on the scenario with non-vanishing non-linear parameters, as their presence does not significantly alter the depicted curves in this figure.

5 Conclusion

In this paper, we investigated how the ModMax-de Sitter black hole reacts when disturbed by a neutral massless scalar field. We began by introducing the radial perturbation equation along with its respective boundary conditions. Then, within the eikonal limit, we derived the quasinormal resonance frequency explicitly for the combined system consisting of the black hole and the neutral massless scalar field. Next, we analyzed how the relaxation behavior of the system changes under scenarios with and without a cosmological constant.

Our findings revealed an interesting trend: as the cosmological constant increases, the fastest relaxation rate also tends to increase. Furthermore, for a specific non-linear parameter value, we noticed that the minimum relaxation time increases as the cosmological constant grows. This result is expected since a similar outcome is reached for the case of RNdS spacetime in four dimensions [42]. Moreover, when the cosmological constant is zero, we observe that the critical values of the black hole charge, determining the minimum relaxation time, also increase with a larger non-linear parameter. This phenomenon arises from the shielding effect exerted by the non-linear parameter on the effective charge of the black hole.

In this study, we thoroughly examine the accuracy of our WKB approximation. In the appendix,

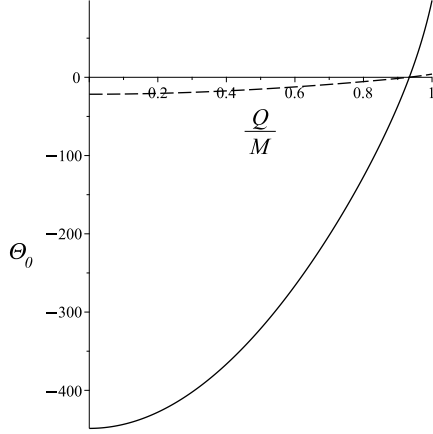


Figure 4.2: Here are numerical examples of Θ_0 for some small L^* . The solid line represents $L^* = 1$, the dashed line represents $L^* = 2$.

we provide all the terms contributing to the complete resonance formula of Iyer and Will [40, 41]. We demonstrate that the calculation for obtaining the relaxation time in section 3 remains valid as long as we consider $l \gg 1$.

For our future research, we plan to explore the resonances of charged massive scalar fields within the context of a charged ModMax black hole. If necessary, we will explore the large-mass regime to simplify the WKB resonance condition for obtaining the real and imaginary parts of the scalar frequency, as suggested in previous studies [36]. Moreover, addressing such a problem in the ModMax-de Sitter background presents an intriguing challenge that deserves further investigation.

Acknowledgement

I thank the anonymous referees for their valuable comments. This work is supported by Kemendikbudristek.

A Coefficients in Π_n and Ω_n series

The followings are the coefficients β_j 's in equation (4.5)

$$\beta_0 = -144 F_0^4 (30n - 1 + 30n^2) ,$$

$$\beta_1 = 728 F_0^3 F_0^{[1]} (1 + 10n + 10n^2) ,$$

$$\beta_2 = 36 F_0^2 \left(32 F_0 F_0^{[2]} - 107 F_0^{[1]2} - 630 F_0^{[1]2} n - 630 F_0^{[1]2} n^2 \right) ,$$

$$\beta_3 = 24 F_0 \left(24 F_0^2 F_0^{[3]} n^2 + 24 F_0^2 F_0^{[3]} n + 4 F_0^2 F_0^{[3]} + 126 F_0 F_0^{[2]} n^2 F_0^{[1]} + 126 F_0 F_0^{[2]} n F_0^{[1]} \right. \\ \left. - 33 F_0 F_0^{[1]} F_0^{[2]} + 108 F_0^{[1]3} + 504 F_0^{[1]3} n + 504 F_0^{[1]3} n^2 \right) ,$$

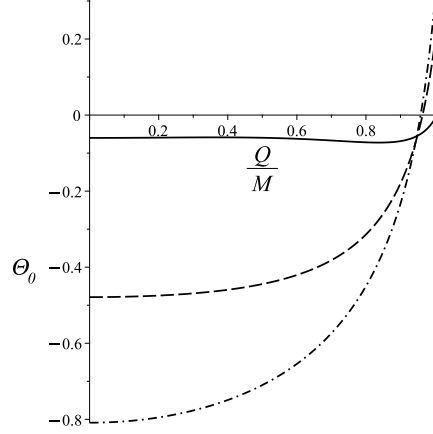


Figure 4.3: Another numerical example of Θ_0 for larger L^* . The solid line represents $L = 5$, the dashed line represents $L = 10$, and the dashed-dot line represents $L = 100$. Again, for higher L , the curves will nearly overlap with the $L = 100$ case.

$$\begin{aligned} \beta_4 = & -3600 F_0 n F_0^{[2]} F_0^{[1]^2} - 936 F_0^{[1]} F_0^2 F_0^{[3]} n + 108 F_0^3 F_0^{[4]} n - 576 F_0^{[1]^4} - 2304 n^2 F_0^{[1]^4} + 108 F_0^3 F_0^{[4]} n^2 \\ & + 54 F_0^3 F_0^{[4]} - 3600 F_0 n^2 F_0^{[2]} F_0^{[1]^2} - 2304 n F_0^{[1]^4} - 936 F_0^{[1]} F_0^2 F_0^{[3]} n^2 + 432 F_0^2 n^2 F_0^{[2]^2} \\ & - 360 F_0 F_0^{[1]^2} F_0^{[2]} + 360 F_0^2 F_0^{[2]^2} - 180 F_0^{[1]} F_0^2 F_0^{[3]} + 432 F_0^2 n F_0^{[2]^2}, \end{aligned}$$

$$\begin{aligned} \beta_5 = & 216 F_0^2 F_0^{[3]} n F_0^{[2]} - 144 F_0 F_0^{[2]^2} n F_0^{[1]} + 1152 F_0^{[2]} n F_0^{[1]^3} - 72 F_0^2 F_0^{[1]} F_0^{[4]} n^2 - 216 F_0 F_0^{[2]^2} F_0^{[1]} \\ & + 288 F_0^{[1]^2} F_0 F_0^{[3]} n^2 + 48 F_0^{[1]^2} F_0 F_0^{[3]} + 60 F_0^2 F_0^{[3]} F_0^{[2]} + 288 F_0^{[2]} F_0^{[1]^3} - 36 F_0^2 F_0^{[1]} F_0^{[4]} \\ & - 144 F_0 F_0^{[2]^2} n^2 F_0^{[1]} - 72 F_0^2 F_0^{[1]} F_0^{[4]} n + 288 F_0^{[1]^2} F_0 F_0^{[3]} n + 1152 F_0^{[2]} n^2 F_0^{[1]^3} + 216 F_0^2 F_0^{[3]} n^2 F_0^{[2]}, \end{aligned}$$

$$\begin{aligned} \beta_6 = & 72 F_0 F_0^{[2]^3} n + 9 F_0^2 F_0^{[4]} F_0^{[2]} - 30 F_0^2 F_0^{[3]^2} n - 144 n F_0^{[2]^2} F_0^{[1]^2} - 36 F_0^{[1]^2} F_0^{[2]^2} - 144 n^2 F_0^{[2]^2} F_0^{[1]^2} \\ & + 36 F_0^{[2]^3} F_0 - 11 F_0^2 F_0^{[3]^2} - 30 F_0^2 F_0^{[3]^2} n^2 - 72 F_0^{[1]} F_0 F_0^{[3]} n^2 F_0^{[2]} + 18 F_0^2 F_0^{[4]} n F_0^{[2]} \\ & + 18 F_0^2 F_0^{[4]} n^2 F_0^{[2]} - 12 F_0^{[1]} F_0 F_0^{[3]} F_0^{[2]} + 72 F_0 F_0^{[2]^3} n^2 - 72 F_0^{[1]} F_0 F_0^{[3]} n F_0^{[2]}, \end{aligned}$$

and γ_j 's in equations (4.6)

$$\gamma_0 = 103680 F_0^7 (37 n^2 + 37 n - 1),$$

$$\gamma_1 = -207360 F_0^{[1]} F_0^6 (-3 + 106 n^2 + 106 n),$$

$$\gamma_2 = 17280 F_0^5 \left(504 F_0 F_0^{[2]} n^2 + 504 F_0 F_0^{[2]} n + 84 F_0 F_0^{[2]} + 3055 F_0^{[1]^2} n^2 - 81 F_0^{[1]^2} + 3055 F_0^{[1]^2} n \right),$$

$$\begin{aligned} \gamma_3 = & -6912 F_0^4 \left(-187 F_0^2 F_0^{[3]} - 230 F_0^2 F_0^{[3]} n^2 - 230 F_0^2 F_0^{[3]} n + 5495 F_0 F_0^{[2]} n F_0^{[1]} \right. \\ & \left. + 5495 F_0 F_0^{[2]} n^2 F_0^{[1]} + 672 F_0 F_0^{[1]} F_0^{[2]} - 222 F_0^{[1]^3} + 10010 F_0^{[1]^3} n + 10010 F_0^{[1]^3} n^2 \right), \end{aligned}$$

$$\begin{aligned} \gamma_4 = & 432 F_0^3 \left(2124 F_0^3 F_0^{[4]} + 3012 F_0^3 F_0^{[4]} n^2 + 3012 F_0^3 F_0^{[4]} n - 11096 F_0^{[1]} F_0^2 F_0^{[3]} n - 8952 F_0^{[1]} F_0^2 F_0^{[3]} \right. \\ & - 11096 F_0^{[1]} F_0^2 F_0^{[3]} n^2 + 3336 F_0^2 F_0^{[2]^2} + 12448 F_0^2 n^2 F_0^{[2]^2} + 12448 F_0^2 n F_0^{[2]^2} + 158272 F_0 n F_0^{[2]} F_0^{[1]^2} \\ & \left. + 13624 F_0 F_0^{[1]^2} F_0^{[2]} + 158272 F_0 n^2 F_0^{[2]} F_0^{[1]^2} - 1961 F_0^{[1]^4} + 124167 n^2 F_0^{[1]^4} + 124167 n F_0^{[1]^4} \right), \end{aligned}$$

$$\begin{aligned} \gamma_5 = & -576 F_0^2 \left(3330 F_0^3 F_0^{[1]} F_0^{[4]} - 144 F_0^4 F_0^{[5]} n^2 - 144 F_0^4 F_0^{[5]} n - 72 F_0^4 F_0^{[5]} - 1410 F_0^3 n F_0^{[2]} F_0^{[3]} \right. \\ & + 5694 F_0^3 F_0^{[1]} F_0^{[4]} n^2 - 1476 F_0^3 F_0^{[2]} F_0^{[3]} - 1410 F_0^3 n^2 F_0^{[2]} F_0^{[3]} + 5694 F_0^3 F_0^{[1]} F_0^{[4]} n \\ & - 9452 F_0^{[1]^2} F_0^2 F_0^{[3]} n^2 + 6306 F_0^2 F_0^{[1]} F_0^{[2]^2} - 7800 F_0^{[1]^2} F_0^2 F_0^{[3]} - 9452 F_0^{[1]^2} F_0^2 F_0^{[3]} n \\ & + 31416 F_0^2 F_0^{[1]} n^2 F_0^{[2]^2} + 31416 F_0^2 F_0^{[1]} n F_0^{[2]^2} + 6549 F_0 F_0^{[2]} F_0^{[1]^3} + 113319 F_0 F_0^{[2]} n F_0^{[1]^3} \\ & \left. + 113319 F_0 F_0^{[2]} n^2 F_0^{[1]^3} - 360 F_0^{[1]^5} + 42804 F_0^{[1]^5} n + 42804 F_0^{[1]^5} n^2 \right), \end{aligned}$$

$$\begin{aligned} \gamma_6 = & 144 F_0 \left(9576 F_0^3 n^2 F_0^{[2]^3} - 13000 F_0^3 F_0^{[3]} F_0^{[2]} F_0^{[1]} n^2 - 13000 F_0^3 F_0^{[3]} F_0^{[2]} F_0^{[1]} n \right. \\ & + 8781 F_0^3 F_0^{[1]^2} F_0^{[4]} + 36 F_0^5 F_0^{[6]} n^2 + 23952 F_0^{[1]^2} F_0^{[2]^2} F_0^2 + 36 F_0^5 F_0^{[6]} n - 17246 F_0^{[1]^3} F_0^2 F_0^{[3]} \\ & + 4698 F_0^4 F_0^{[2]} F_0^{[4]} - 246 F_0^4 F_0^{[3]^2} n - 546 F_0^{[1]} F_0^4 F_0^{[5]} - 246 F_0^4 F_0^{[3]^2} n^2 + 8856 F_0^{[2]} F_0^{[1]^4} F_0 \\ & + 168912 F_0^2 n F_0^{[2]^2} F_0^{[1]^2} + 168912 F_0^2 n^2 F_0^{[2]^2} F_0^{[1]^2} + 242532 F_0 F_0^{[1]^4} F_0^{[2]} n^2 \\ & - 18450 F_0^{[1]^3} F_0^2 F_0^{[3]} n^2 - 18450 F_0^{[1]^3} F_0^2 F_0^{[3]} n - 13608 F_0^3 F_0^{[1]} F_0^{[3]} F_0^{[2]} \\ & + 20591 F_0^3 F_0^{[1]^2} F_0^{[4]} n + 6234 F_0^4 F_0^{[2]} F_0^{[4]} n^2 + 6234 F_0^4 F_0^{[2]} F_0^{[4]} n - 1452 F_0^{[1]} F_0^4 F_0^{[5]} n^2 \\ & - 1452 F_0^{[1]} F_0^4 F_0^{[5]} n + 9576 F_0^3 n F_0^{[2]^3} + 242532 F_0 F_0^{[1]^4} F_0^{[2]} n + 20591 F_0^3 F_0^{[1]^2} F_0^{[4]} n^2 \\ & \left. - 96 F_0^{[1]^6} + 43200 F_0^{[1]^6} n^2 + 43200 F_0^{[1]^6} n + 3432 F_0^3 F_0^{[2]^3} - 246 F_0^4 F_0^{[3]^2} + 54 F_0^5 F_0^{[6]} \right), \end{aligned}$$

$$\begin{aligned} \gamma_7 = & 1405728 F_0^3 F_0^{[3]} F_0^{[1]^2} F_0^{[2]} n^2 - 1584288 F_0^4 F_0^{[2]} F_0^{[1]} F_0^{[4]} n^2 - 1584288 F_0^4 F_0^{[2]} F_0^{[1]} F_0^{[4]} n \\ & + 1405728 F_0^3 F_0^{[3]} F_0^{[1]^2} F_0^{[2]} n + 56448 F_0^4 F_0^{[3]^2} F_0^{[1]} n + 300672 F_0^{[1]^4} F_0^2 F_0^{[3]} n^2 \\ & + 1593504 F_0^3 F_0^{[3]} F_0^{[1]^2} F_0^{[2]} - 1094688 F_0^3 F_0^{[1]^3} F_0^{[4]} n^2 - 1094688 F_0^3 F_0^{[1]^3} F_0^{[4]} n \\ & + 622080 F_0^{[1]^4} F_0^2 F_0^{[3]} + 39168 F_0^4 F_0^{[1]^2} F_0^{[5]} - 189792 F_0^3 F_0^{[1]^3} F_0^{[4]} - 15552 F_0^5 F_0^{[6]} F_0^{[1]} \\ & - 62208 F_0^5 F_0^{[3]} F_0^{[4]} + 229824 F_0^4 F_0^{[3]} F_0^{[2]^2} - 186624 F_0^{[1]^5} F_0 F_0^{[2]} + 31968 F_0^5 F_0^{[2]} F_0^{[5]} \\ & + 65664 F_0^4 F_0^{[3]^2} F_0^{[1]} - 100224 F_0^5 F_0^{[3]} F_0^{[4]} n^2 - 100224 F_0^5 F_0^{[3]} F_0^{[4]} n + 188928 F_0^4 F_0^{[1]^2} F_0^{[5]} n^2 \\ & + 188928 F_0^4 F_0^{[1]^2} F_0^{[5]} n + 53568 F_0^5 F_0^{[2]} F_0^{[5]} n^2 + 53568 F_0^5 F_0^{[2]} F_0^{[5]} n - 16386624 F_0^{[2]^2} F_0^{[1]^3} F_0^2 n^2 \\ & - 9911808 F_0^{[1]^5} F_0 F_0^{[2]} n^2 - 9911808 F_0^{[1]^5} F_0 F_0^{[2]} n - 3462912 F_0^3 F_0^{[2]^3} F_0^{[1]} n^2 - 3462912 F_0^3 F_0^{[2]^3} F_0^{[1]} n \end{aligned}$$

$$\begin{aligned}
& + 56448 F_0^4 F_0^{[3]^2} F_0^{[1]} n^2 - 663552 F_0^{[1]^7} n^2 - 663552 F_0^{[1]^7} n + 180864 F_0^4 F_0^{[3]} F_0^{[2]^2} n^2 \\
& + 180864 F_0^4 F_0^{[3]} F_0^{[2]^2} n - 10368 F_0^5 F_0^{[6]} n F_0^{[1]} - 16386624 F_0^{[2]^2} F_0^{[1]^3} F_0^2 n - 917568 F_0^3 F_0^{[2]^3} F_0^{[1]} \\
& + 300672 F_0^{[1]^4} F_0^2 F_0^{[3]} n - 982368 F_0^4 F_0^{[2]} F_0^{[1]} F_0^{[4]} - 10368 F_0^5 F_0^{[6]} n^2 F_0^{[1]} - 1513728 F_0^{[2]^2} F_0^{[1]^3} F_0^2, \\
\gamma_8 = & -1836 F_0^5 F_0^{[4]^2} n^2 + 155520 F_0^3 F_0^{[2]^4} n - 50688 F_0^{[1]^5} F_0 F_0^{[3]} - 18144 F_0^4 F_0^{[3]^2} F_0^{[2]} + 3888 F_0^5 F_0^{[6]} F_0^{[2]} \\
& - 37224 F_0^3 F_0^{[3]^2} F_0^{[1]^2} + 10368 F_0^4 F_0^{[6]} F_0^{[1]^2} + 1161216 F_0^{[1]^6} F_0^{[2]} n^2 - 1836 F_0^5 F_0^{[4]^2} n \\
& + 3456 F_0^3 F_0^{[1]^3} F_0^{[5]} + 599616 F_0^{[2]^3} F_0^{[1]^2} F_0^2 + 172800 F_0^4 F_0^{[2]^2} F_0^{[4]} + 155520 F_0^3 F_0^{[2]^4} n^2 \\
& - 5616 F_0^5 F_0^{[3]} F_0^{[5]} - 62208 F_0^{[1]^4} F_0^2 F_0^{[4]} - 71424 F_0^3 F_0^{[1]^3} F_0^{[5]} n^2 + 209376 F_0^4 F_0^{[2]^2} F_0^{[4]} n \\
& + 156672 F_0^{[1]^5} F_0 F_0^{[3]} n^2 - 11688 F_0^3 F_0^{[3]^2} F_0^{[1]^2} n + 2592 F_0^5 F_0^{[6]} n^2 F_0^{[2]} + 112896 F_0^{[1]^4} F_0^2 F_0^{[4]} n^2 \\
& + 209376 F_0^4 F_0^{[2]^2} F_0^{[4]} n^2 - 11688 F_0^3 F_0^{[3]^2} F_0^{[1]^2} n^2 + 5503680 F_0^{[2]^2} F_0^{[1]^4} F_0 n + 3301344 F_0^{[2]^3} F_0^{[1]^2} F_0^2 n^2 \\
& - 382464 F_0^3 F_0^{[2]^2} F_0^{[1]} F_0^{[3]} + 2592 F_0^5 F_0^{[6]} n F_0^{[2]} - 30528 F_0^4 F_0^{[3]^2} F_0^{[2]} n + 6912 F_0^4 F_0^{[6]} n^2 F_0^{[1]^2} \\
& + 81648 F_0^4 F_0^{[3]} F_0^{[1]} F_0^{[4]} + 6912 F_0^4 F_0^{[6]} n F_0^{[1]^2} - 38592 F_0^{[1]} F_0^4 F_0^{[5]} F_0^{[2]} + 348696 F_0^{[1]^2} F_0^{[2]} F_0^3 F_0^{[4]} \\
& + 3301344 F_0^{[2]^3} F_0^{[1]^2} F_0^2 n - 71424 F_0^3 F_0^{[1]^3} F_0^{[5]} n - 6048 F_0^5 F_0^{[3]} F_0^{[5]} n - 491904 F_0^{[2]} F_0^{[1]^3} F_0^2 F_0^{[3]} \\
& + 5503680 F_0^{[2]^2} F_0^{[1]^4} F_0 n^2 + 75168 F_0^3 F_0^{[2]^4} - 2268 F_0^5 F_0^{[4]^2} - 234144 F_0^{[2]} F_0^{[1]^3} F_0^2 F_0^{[3]} n \\
& - 297216 F_0^3 F_0^{[2]^2} F_0^{[1]} F_0^{[3]} n^2 - 297216 F_0^3 F_0^{[2]^2} F_0^{[1]} F_0^{[3]} n + 852552 F_0^{[1]^2} F_0^{[2]} F_0^3 F_0^{[4]} n \\
& + 159120 F_0^4 F_0^{[3]} F_0^{[1]} F_0^{[4]} n^2 + 159120 F_0^4 F_0^{[3]} F_0^{[1]} F_0^{[4]} n - 91008 F_0^{[1]} F_0^4 F_0^{[5]} F_0^{[2]} n^2 \\
& + 261792 F_0^{[2]^2} F_0^{[1]^4} F_0 + 1161216 F_0^{[1]^6} F_0^{[2]} n + 112896 F_0^{[1]^4} F_0^2 F_0^{[4]} n + 156672 F_0^{[1]^5} F_0 F_0^{[3]} n \\
& - 30528 F_0^4 F_0^{[3]^2} F_0^{[2]} n^2 - 6048 F_0^5 F_0^{[3]} F_0^{[5]} n^2 - 234144 F_0^{[2]} F_0^{[1]^3} F_0^2 F_0^{[3]} n^2 \\
& - 91008 F_0^{[1]} F_0^4 F_0^{[5]} F_0^{[2]} n + 852552 F_0^{[1]^2} F_0^{[2]} F_0^3 F_0^{[4]} n^2, \\
\gamma_9 = & 7200 F_0^4 F_0^{[2]^2} F_0^{[5]} - 136512 F_0^{[2]^3} F_0^{[1]^3} F_0 - 732672 F_0^{[2]^2} F_0^{[1]^5} n^2 - 4608 F_0^{[1]^4} F_0^2 F_0^{[5]} \\
& - 2304 F_0^3 F_0^{[6]} F_0^{[1]^3} - 100224 F_0^2 F_0^{[2]^4} F_0^{[1]} - 1392768 F_0^{[2]^3} F_0^{[1]^3} F_0 n - 1392768 F_0^{[2]^3} F_0^{[1]^3} F_0 n^2 \\
& + 84672 F_0^{[1]^2} F_0^{[2]^2} F_0^2 F_0^{[3]} n^2 + 84672 F_0^{[1]^2} F_0^{[2]^2} F_0^2 F_0^{[3]} n + 46704 F_0^3 F_0^{[3]^2} F_0^{[2]} F_0^{[1]} n^2 \\
& - 105984 F_0^{[2]} F_0^{[1]^4} F_0 F_0^{[3]} n^2 - 105984 F_0^{[2]} F_0^{[1]^4} F_0 F_0^{[3]} n - 118656 F_0^{[2]} F_0^{[1]^3} F_0^2 F_0^{[4]} n^2 \\
& - 213840 F_0^3 F_0^{[2]^2} F_0^{[1]} F_0^{[4]} n^2 - 213840 F_0^3 F_0^{[2]^2} F_0^{[1]} F_0^{[4]} n - 71328 F_0^3 F_0^{[3]} F_0^{[1]^2} F_0^{[4]} n^2 \\
& - 44208 F_0^4 F_0^{[3]} F_0^{[2]} F_0^{[4]} n^2 - 44208 F_0^4 F_0^{[3]} F_0^{[2]} F_0^{[4]} n + 47232 F_0^{[1]^2} F_0^3 F_0^{[5]} F_0^{[2]} n^2 \\
& + 8064 F_0^4 F_0^{[3]} F_0^{[5]} n^2 F_0^{[1]} + 8064 F_0^4 F_0^{[3]} F_0^{[5]} n F_0^{[1]} - 3456 F_0^4 F_0^{[6]} n^2 F_0^{[2]} F_0^{[1]} \\
& + 37728 F_0^3 F_0^{[3]} F_0^{[2]^3} - 36864 F_0^{[1]^6} F_0^{[3]} n - 384 F_0^2 F_0^{[3]^2} F_0^{[1]^3} + 960 F_0^4 F_0^{[3]^3} n
\end{aligned}$$

$$\begin{aligned}
& - 36864 F_0^{[1]6} F_0^{[3]} n^2 - 278208 F_0^2 F_0^{[2]4} F_0^{[1]} n - 278208 F_0^2 F_0^{[2]4} F_0^{[1]} n^2 + 39168 F_0^{[2]} F_0^{[1]4} F_0 F_0^{[3]} \\
& + 27648 F_0^3 F_0^{[3]} F_0^{[2]3} n + 30672 F_0^3 F_0^{[3]2} F_0^{[2]} F_0^{[1]} - 25536 F_0^2 F_0^{[3]2} F_0^{[1]3} n + 27648 F_0^3 F_0^{[3]} F_0^{[2]3} n^2 \\
& + 162432 F_0^{[1]2} F_0^{[2]2} F_0^2 F_0^{[3]} + 2448 F_0^4 F_0^{[4]2} n F_0^{[1]} + 2448 F_0^4 F_0^{[4]2} n^2 F_0^{[1]} + 9216 F_0^{[1]5} F_0 F_0^{[4]} n^2 \\
& - 142704 F_0^3 F_0^{[2]2} F_0^{[1]} F_0^{[4]} + 14976 F_0^{[2]} F_0^{[1]3} F_0^2 F_0^{[4]} - 20448 F_0^3 F_0^{[3]} F_0^{[1]2} F_0^{[4]} - 28944 F_0^4 F_0^{[3]} F_0^{[2]} F_0^{[4]} \\
& + 9216 F_0^{[1]4} F_0^2 F_0^{[5]} n^2 + 10944 F_0^4 F_0^{[2]2} F_0^{[5]} n + 9216 F_0^{[1]4} F_0^2 F_0^{[5]} n + 10944 F_0^4 F_0^{[2]2} F_0^{[5]} n^2 \\
& + 7488 F_0^4 F_0^{[3]} F_0^{[5]} F_0^{[1]} - 1536 F_0^3 F_0^{[6]} n F_0^{[1]3} - 1536 F_0^3 F_0^{[6]} n^2 F_0^{[1]3} - 5184 F_0^4 F_0^{[6]} F_0^{[2]} F_0^{[1]}, \\
\gamma_{10} = & 36168 F_0^3 F_0^{[1]} F_0^{[3]} F_0^{[2]} F_0^{[4]} n^2 + 36168 F_0^3 F_0^{[1]} F_0^{[3]} F_0^{[2]} F_0^{[4]} n - 1008 F_0^3 F_0^{[4]2} F_0^{[1]2} \\
& + 6912 F_0^2 F_0^{[2]5} n - 756 F_0^4 F_0^{[4]2} F_0^{[2]} + 217728 F_0^{[2]3} F_0^{[1]4} n^2 + 2052 F_0^4 F_0^{[3]2} F_0^{[4]} + 217728 F_0^{[2]3} F_0^{[1]4} n \\
& + 2688 F_0^{[1]4} F_0 F_0^{[3]2} + 648 F_0^4 F_0^{[6]} F_0^{[2]2} + 16848 F_0^3 F_0^{[2]3} F_0^{[4]} + 936 F_0^3 F_0^{[3]3} F_0^{[1]} + 34560 F_0^{[2]4} F_0^{[1]2} F_0 \\
& + 6048 F_0^2 F_0^{[2]5} - 14688 F_0^{[1]} F_0^2 F_0^{[3]} F_0^{[2]3} n + 23616 F_0^{[1]3} F_0^{[2]2} F_0 F_0^{[3]} n^2 + 23616 F_0^{[1]3} F_0^{[2]2} F_0 F_0^{[3]} n \\
& - 2640 F_0^2 F_0^{[3]2} F_0^{[1]2} F_0^{[2]} n^2 - 2640 F_0^2 F_0^{[3]2} F_0^{[1]2} F_0^{[2]} n - 14688 F_0^{[1]} F_0^2 F_0^{[3]} F_0^{[2]3} n^2 \\
& - 6912 F_0^{[2]} F_0^{[1]4} F_0 F_0^{[4]} n^2 - 6912 F_0^{[2]} F_0^{[1]4} F_0 F_0^{[4]} n + 41616 F_0^{[1]2} F_0^{[2]2} F_0^2 F_0^{[4]} n^2 \\
& + 6528 F_0^{[1]3} F_0^2 F_0^{[3]} F_0^{[4]} n^2 + 6528 F_0^{[1]3} F_0^2 F_0^{[3]} F_0^{[4]} n + 17496 F_0^3 F_0^{[1]} F_0^{[3]} F_0^{[2]} F_0^{[4]} \\
& - 6912 F_0^{[1]3} F_0^2 F_0^{[5]} F_0^{[2]} n^2 - 10224 F_0^{[1]} F_0^3 F_0^{[5]} F_0^{[2]2} n - 6912 F_0^{[1]3} F_0^2 F_0^{[5]} F_0^{[2]} n \\
& - 2688 F_0^3 F_0^{[3]} F_0^{[5]} n F_0^{[1]2} - 2016 F_0^4 F_0^{[3]} F_0^{[5]} n^2 F_0^{[2]} - 2016 F_0^4 F_0^{[3]} F_0^{[5]} n F_0^{[2]} \\
& + 1152 F_0^3 F_0^{[6]} n F_0^{[1]2} F_0^{[2]} + 162432 F_0^{[2]4} F_0^{[1]2} F_0 n^2 + 162432 F_0^{[2]4} F_0^{[1]2} F_0 n + 9984 F_0^{[1]4} F_0 F_0^{[3]2} n^2 \\
& - 3240 F_0^3 F_0^{[3]3} F_0^{[1]} n^2 - 3240 F_0^3 F_0^{[3]3} F_0^{[1]} n - 11904 F_0^3 F_0^{[3]2} F_0^{[2]2} n^2 - 11904 F_0^3 F_0^{[3]2} F_0^{[2]2} n \\
& + 27648 F_0^{[2]} F_0^{[1]5} F_0^{[3]} n^2 + 27648 F_0^{[2]} F_0^{[1]5} F_0^{[3]} n - 12384 F_0^{[1]3} F_0^{[2]2} F_0 F_0^{[3]} - 5280 F_0^2 F_0^{[3]2} F_0^{[1]2} F_0^{[2]} \\
& - 27648 F_0^{[1]} F_0^2 F_0^{[3]} F_0^{[2]3} - 816 F_0^3 F_0^{[4]2} n^2 F_0^{[1]2} - 816 F_0^3 F_0^{[4]2} n F_0^{[1]2} + 17280 F_0^3 F_0^{[2]3} F_0^{[4]} n^2 \\
& - 612 F_0^4 F_0^{[4]2} n^2 F_0^{[2]} - 612 F_0^4 F_0^{[4]2} n F_0^{[2]} - 6912 F_0^{[2]} F_0^{[1]4} F_0 F_0^{[4]} + 11088 F_0^{[1]2} F_0^{[2]2} F_0^2 F_0^{[4]} \\
& + 2700 F_0^4 F_0^{[3]2} F_0^{[4]} n - 4224 F_0^{[1]3} F_0^2 F_0^{[3]} F_0^{[4]} + 3456 F_0^{[1]3} F_0^2 F_0^{[5]} F_0^{[2]} - 3816 F_0^{[1]} F_0^3 F_0^{[5]} F_0^{[2]2} \\
& - 1872 F_0^4 F_0^{[3]} F_0^{[5]} F_0^{[2]} + 432 F_0^4 F_0^{[6]} n^2 F_0^{[2]2} + 432 F_0^4 F_0^{[6]} n F_0^{[2]2} + 1728 F_0^3 F_0^{[6]} F_0^{[1]2} F_0^{[2]} \\
& - 732672 F_0^{[2]2} F_0^{[1]5} n - 1536 F_0^4 F_0^{[3]3} + 46704 F_0^3 F_0^{[3]2} F_0^{[2]} F_0^{[1]} n - 118656 F_0^{[2]} F_0^{[1]3} F_0^2 F_0^{[4]} n \\
& - 71328 F_0^3 F_0^{[3]} F_0^{[1]2} F_0^{[4]} n + 47232 F_0^{[1]2} F_0^3 F_0^{[5]} F_0^{[2]} n - 3456 F_0^4 F_0^{[6]} n F_0^{[2]} F_0^{[1]} + 960 F_0^4 F_0^{[3]3} n^2 \\
& + 3024 F_0^4 F_0^{[4]2} F_0^{[1]} + 9216 F_0^{[1]5} F_0 F_0^{[4]} - 25536 F_0^2 F_0^{[3]2} F_0^{[1]3} n^2 + 9216 F_0^{[1]5} F_0 F_0^{[4]} n \\
& + 6336 F_0^{[1]2} F_0^3 F_0^{[5]} F_0^{[2]} - 8352 F_0^3 F_0^{[3]2} F_0^{[2]2} + 6912 F_0^2 F_0^{[2]5} n^2 + 41616 F_0^{[1]2} F_0^{[2]2} F_0^2 F_0^{[4]} n
\end{aligned}$$

$$\begin{aligned}
& - 10224 F_0^{[1]} F_0^3 F_0^{[5]} F_0^{[2]^2} n^2 - 2688 F_0^3 F_0^{[3]} F_0^{[5]} n^2 F_0^{[1]^2} + 1152 F_0^3 F_0^{[6]} n^2 F_0^{[1]^2} F_0^{[2]} \\
& + 9984 F_0^{[1]^4} F_0 F_0^{[3]^2} n + 17280 F_0^3 F_0^{[2]^3} F_0^{[4]} n + 2700 F_0^4 F_0^{[3]^2} F_0^{[4]} n^2 - 2496 F_0^3 F_0^{[3]} F_0^{[5]} F_0^{[1]^2}, \\
\gamma_{11} = & - 3264 F_0^{[1]^2} F_0^2 F_0^{[3]} F_0^{[2]} F_0^{[4]} n^2 - 3264 F_0^{[1]^2} F_0^2 F_0^{[3]} F_0^{[2]} F_0^{[4]} n + 1344 F_0^3 F_0^{[3]} F_0^{[5]} n^2 F_0^{[1]} F_0^{[2]} \\
& + 1344 F_0^3 F_0^{[3]} F_0^{[5]} n F_0^{[1]} F_0^{[2]} + 504 F_0^3 F_0^{[2]^3} F_0^{[5]} - 4320 F_0 F_0^{[2]^5} F_0^{[1]} + 984 F_0^3 F_0^{[3]^3} F_0^{[2]} \\
& - 768 F_0^{[1]^2} F_0^2 F_0^{[3]^3} - 31104 F_0^{[1]^3} F_0^{[2]^4} n^2 - 31104 F_0^{[1]^3} F_0^{[2]^4} n - 4992 F_0 F_0^{[2]} F_0^{[1]^3} F_0^{[3]^2} n^2 \\
& + 3696 F_0^2 F_0^{[1]} F_0^{[2]^2} F_0^{[3]^2} n^2 + 3696 F_0^2 F_0^{[1]} F_0^{[2]^2} F_0^{[3]^2} n - 1728 F_0^{[2]^3} F_0^{[1]^2} F_0 F_0^{[3]} n^2 n \\
& + 1728 F_0^{[1]^3} F_0^{[2]^2} F_0 F_0^{[4]} n - 5616 F_0^2 F_0^{[2]^3} F_0^{[1]} F_0^{[4]} n^2 - 5616 F_0^2 F_0^{[2]^3} F_0^{[1]} F_0^{[4]} n \\
& + 408 F_0^3 F_0^{[4]^2} n^2 F_0^{[1]} F_0^{[2]} + 408 F_0^3 F_0^{[4]^2} n F_0^{[1]} F_0^{[2]} - 1800 F_0^3 F_0^{[3]^2} F_0^{[4]} n^2 F_0^{[1]} \\
& - 4584 F_0^3 F_0^{[3]} F_0^{[2]^2} F_0^{[4]} n^2 - 4584 F_0^3 F_0^{[3]} F_0^{[2]^2} F_0^{[4]} n + 2112 F_0^{[1]^2} F_0^2 F_0^{[3]} F_0^{[2]} F_0^{[4]} \\
& + 1728 F_0^{[1]^2} F_0^2 F_0^{[5]} F_0^{[2]^2} n^2 + 1728 F_0^{[1]^2} F_0^2 F_0^{[5]} F_0^{[2]^2} n + 1248 F_0^3 F_0^{[3]} F_0^{[5]} F_0^{[1]} F_0^{[2]} \\
& - 288 F_0^3 F_0^{[6]} n F_0^{[2]^2} F_0^{[1]} - 288 F_0^3 F_0^{[6]} n^2 F_0^{[2]^2} F_0^{[1]} - 6912 F_0 F_0^{[2]^5} F_0^{[1]} n^2 - 6912 F_0 F_0^{[2]^5} F_0^{[1]} n \\
& + 480 F_0^{[1]^2} F_0^2 F_0^{[3]^3} n^2 + 480 F_0^{[1]^2} F_0^2 F_0^{[3]^3} n + 2040 F_0^3 F_0^{[3]^3} F_0^{[2]} n^2 + 2040 F_0^3 F_0^{[3]^3} F_0^{[2]} n \\
& + 864 F_0^2 F_0^{[3]} F_0^{[2]^4} n^2 + 864 F_0^2 F_0^{[3]} F_0^{[2]^4} n - 6912 F_0^{[2]^2} F_0^{[1]^4} F_0^{[3]} n^2 - 6912 F_0^{[2]^2} F_0^{[1]^4} F_0^{[3]} n \\
& + 3072 F_0^2 F_0^{[1]} F_0^{[2]^2} F_0^{[3]^2} + 2016 F_0^{[2]^3} F_0^{[1]^2} F_0 F_0^{[3]} + 1728 F_0^{[1]^3} F_0^{[2]^2} F_0 F_0^{[4]} - 4464 F_0^2 F_0^{[2]^3} F_0^{[1]} F_0^{[4]} \\
& - 1368 F_0^3 F_0^{[3]^2} F_0^{[4]} F_0^{[1]} - 3096 F_0^3 F_0^{[3]} F_0^{[2]^2} F_0^{[4]} + 720 F_0^3 F_0^{[2]^3} F_0^{[5]} n^2 + 720 F_0^3 F_0^{[2]^3} F_0^{[5]} n \\
& - 864 F_0^{[1]^2} F_0^2 F_0^{[5]} F_0^{[2]^2} - 432 F_0^3 F_0^{[6]} F_0^{[2]^2} F_0^{[1]} + 1728 F_0^{[1]^3} F_0^{[2]^2} F_0 F_0^{[4]} n^2 + 504 F_0^3 F_0^{[4]^2} F_0^{[1]} F_0^{[2]} \\
& + 2016 F_0^2 F_0^{[3]} F_0^{[2]^4} - 4992 F_0 F_0^{[2]} F_0^{[1]^3} F_0^{[3]^2} n - 1728 F_0^{[2]^3} F_0^{[1]^2} F_0 F_0^{[3]} - 1800 F_0^3 F_0^{[3]^2} F_0^{[4]} n F_0^{[1]} \\
& - 1344 F_0 F_0^{[2]} F_0^{[1]^3} F_0^{[3]^2}, \\
\gamma_{12} = & 408 F_0^{[1]} F_0^2 F_0^{[3]} F_0^{[2]^2} F_0^{[4]} n + 408 F_0^{[1]} F_0^2 F_0^{[3]} F_0^{[2]^2} F_0^{[4]} n^2 - 432 F_0^2 F_0^{[3]^2} F_0^{[2]^3} + 1728 F_0^{[2]^5} F_0^{[1]^2} n^2 \\
& - 235 F_0^3 F_0^{[3]^4} n^2 + 1728 F_0^{[2]^5} F_0^{[1]^2} n - 63 F_0^3 F_0^{[4]^2} F_0^{[2]^2} + 432 F_0^2 F_0^{[2]^4} F_0^{[4]} - 235 F_0^3 F_0^{[3]^4} n \\
& - 144 F_0^{[2]^3} F_0^{[1]^2} F_0 F_0^{[4]} n + 216 F_0 F_0^{[2]^6} - 144 F_0^{[2]^3} F_0^{[1]^2} F_0 F_0^{[4]} n^2 - 264 F_0^{[1]} F_0^2 F_0^{[3]} F_0^{[2]^2} F_0^{[4]} \\
& - 120 F_0^{[1]} F_0^{[2]} F_0^2 F_0^{[3]^3} n - 120 F_0^{[1]} F_0^{[2]} F_0^2 F_0^{[3]^3} n^2 + 450 F_0^3 F_0^{[3]^2} F_0^{[4]} n^2 F_0^{[2]} - 155 F_0^3 F_0^{[3]^4} \\
& - 360 F_0^2 F_0^{[3]^2} F_0^{[2]^3} n + 576 F_0^{[2]^3} F_0^{[1]^3} F_0^{[3]} n^2 + 576 F_0^{[2]^3} F_0^{[1]^3} F_0^{[3]} n + 192 F_0^{[1]} F_0^{[2]} F_0^2 F_0^{[3]^3} \\
& - 144 F_0^{[1]} F_0 F_0^{[3]} F_0^{[2]^4} - 51 F_0^3 F_0^{[4]^2} n^2 F_0^{[2]^2} - 51 F_0^3 F_0^{[4]^2} n F_0^{[2]^2} + 216 F_0^2 F_0^{[2]^4} F_0^{[4]} n^2 \\
& - 144 F_0^{[2]^3} F_0^{[1]^2} F_0 F_0^{[4]} + 342 F_0^3 F_0^{[3]^2} F_0^{[4]} F_0^{[2]} + 72 F_0^2 F_0^{[2]^3} F_0^{[1]} F_0^{[5]} - 156 F_0^3 F_0^{[3]} F_0^{[5]} F_0^{[2]^2} \\
& + 24 F_0^3 F_0^{[6]} n F_0^{[2]^3} + 36 F_0^3 F_0^{[6]} F_0^{[2]^3} + 450 F_0^3 F_0^{[3]^2} F_0^{[4]} n F_0^{[2]} - 168 F_0^3 F_0^{[3]} F_0^{[5]} n F_0^{[2]^2} \\
& - 144 F_0^2 F_0^{[2]^3} F_0^{[1]} F_0^{[5]} n - 168 F_0^3 F_0^{[3]} F_0^{[5]} n^2 F_0^{[2]^2} - 144 F_0^2 F_0^{[2]^3} F_0^{[1]} F_0^{[5]} n^2 + 24 F_0^3 F_0^{[6]} n^2 F_0^{[2]^3} \\
& + 624 F_0^{[1]^2} F_0^{[2]^2} F_0 F_0^{[3]^2} n + 624 F_0^{[1]^2} F_0^{[2]^2} F_0 F_0^{[3]^2} n^2 - 360 F_0^2 F_0^{[3]^2} F_0^{[2]^3} n^2 + 168 F_0^{[1]^2} F_0^{[2]^2} F_0 F_0^{[3]^2} \\
& + 216 F_0^2 F_0^{[2]^4} F_0^{[4]} n.
\end{aligned}$$

References

- [1] M. Born and L. Infeld, Proc. Roy. Soc. Lond. A **144** (1934) no.852, 425-451
- [2] E. S. Fradkin and A. A. Tseytlin, Phys. Lett. B **163** (1985), 123-130
- [3] W. Heisenberg and H. Euler, Z. Phys. **98** (1936) no.11-12, 714-732
- [4] I. Bandos, K. Lechner, D. Sorokin and P. K. Townsend, Phys. Rev. D **102** (2020), 121703
- [5] D. Flores-Alfonso, B. A. González-Morales, R. Linares and M. Maceda, Phys. Lett. B **812** (2021), 136011
- [6] J. Barrientos, A. Cisterna, D. Kubiznak and J. Oliva, Phys. Lett. B **834** (2022), 137447
- [7] A. Ali and K. Saifullah, Annals Phys. **437** (2022), 168726
- [8] S. I. Kruglov, Int. J. Mod. Phys. D **31** (2022) no.04, 2250025
- [9] K. Nomura and D. Yoshida, Phys. Rev. D **105** (2022) no.4, 044006
- [10] S. I. Kruglov, Phys. Lett. B **822** (2021), 136633
- [11] A. Bokulić, T. Jurić and I. Smolić, Phys. Rev. D **103** (2021) no.12, 124059
- [12] D. Flores-Alfonso, R. Linares and M. Maceda, JHEP **09** (2021), 104
- [13] A. Ballon Bordo, D. Kubizňák and T. R. Perche, Phys. Lett. B **817** (2021), 136312
- [14] H. M. Siahaan, Int. J. Mod. Phys. D **32** (2023) no.15, 2350099
- [15] H. M. Siahaan, *to be published in Communications in Theoretical Physics*
- [16] E. Berti, V. Cardoso and A. O. Starinets, Class. Quant. Grav. **26** (2009), 163001
- [17] V. Cardoso, J. L. Costa, K. Destounis, P. Hintz and A. Jansen, Phys. Rev. Lett. **120** (2018) no.3, 031103
- [18] S. Hod, Nucl. Phys. B **941** (2019), 636-645
- [19] S. Hod, Phys. Rev. D **91** (2015) no.4, 044047
- [20] S. Hod, Phys. Rev. D **94** (2016) no.4, 044036
- [21] S. Hod, Phys. Lett. B **763** (2016), 275-279
- [22] S. Hod, Phys. Lett. B **786** (2018), 217 [erratum: Phys. Lett. B **796** (2019), 256]
- [23] S. Hod, Phys. Lett. B **751** (2015), 177-183
- [24] Y. Huang, D. J. Liu, X. H. Zhai and X. Z. Li, Class. Quant. Grav. **34** (2017) no.15, 155002
- [25] R. Li, Y. Zhao, T. Zi and X. Chen, Phys. Rev. D **99** (2019) no.8, 084045

- [26] H. M. Siahaan, *Int. J. Mod. Phys. D* **24** (2015) no.14, 1550102
- [27] H. P. Nollert, *Class. Quant. Grav.* **16** (1999), R159-R216
- [28] V. Cardoso and J. P. S. Lemos, *Phys. Rev. D* **63** (2001), 124015
- [29] S. Hod, *Phys. Rev. Lett.* **81** (1998), 4293
- [30] B. Carter, *Phys. Rev. Lett.* **26** (1971), 331-333
- [31] S. W. Hawking, *Commun. Math. Phys.* **25** (1972), 152-166
- [32] D. C. Robinson, *Phys. Rev. Lett.* **34** (1975), 905-906
- [33] R. Ruffini and J. A. Wheeler, *Phys. Today* **24** (1971) no.1, 30
- [34] Z. Zhu, S. J. Zhang, C. E. Pellicer, B. Wang and E. Abdalla, *Phys. Rev. D* **90** (2014) no.4, 044042
- [35] R. A. Konoplya and A. Zhidenko, *Phys. Rev. D* **90** (2014) no.6, 064048
- [36] S. Hod, *Phys. Lett. B* **761** (2016), 53
- [37] M. Zhang, J. Jiang and Z. Zhong, *Phys. Lett. B* **789** (2019), 13-18
- [38] S. Hod, *Eur. Phys. J. C* **78** (2018) no.11, 935
- [39] M. Zhang, J. Jiang and Z. Zhong, *Phys. Lett. B* **798** (2019), 134959
- [40] S. Iyer and C. M. Will, *Phys. Rev. D* **35** (1987), 3621
- [41] S. Iyer, *Phys. Rev. D* **35** (1987), 3632
- [42] M. Zhang, J. Jiang and Z. Zhong, *Phys. Lett. B* **806** (2020), 135523